Digest Journal of Nanomaterials and Biostructures Vol. 15, No. 2, April - June 2020, p. 345 - 358

EFFECT OF PLASMA SPRAYED α-TRI-CALCIUM PHOSPHATE (α-TCP)DEPOSITION OVER METALLIC BIOMATERIAL SURFACES FOR BIOMEDICAL APPLICATIONS

R. B. DURAIRAJ[a,*], M. NAGARAJ[b], G. MAGESHWARAN[a], G. B. JOESPH[a], V. SRIRAM[a], J. JEEVAHAN[a]
[a]*Assistant Professor, School of Mechanical Engineering, Sathyabama institute of science and Technology, Chennai, India*
[b]*Assistant Professor, Department of Mechanical Engineering, MNM Jain Engineering College, Chennai, India*

Metallic biomaterials are of great interest due to their higher mechanical properties. However, most biological reactions occur at surfaces and interfaces, and the performance of the metallic biomaterials is directly affected by the performance of human body and the biological reactions in the host human body. Most of the metallic biomaterials do not meet the requirements in terms of both surface and bulk properties for biomedical applications. An effective way for making a clinically appealing biomaterial is to introduce surface modification with the biocompatible material to bring the bio functionality onto the surface while the mechanical performance of the base metal is not compromised. α-tri-calcium phosphate (α-TCP) is one of the promising biocompatible ceramic used for biomedical applications. Some of the previous works on α-TCP coatings had discussion on bioactivity and/ or corrosion resistance of the metallic biomaterials. However, there is a little information on the applicability of α-TCP for a variety of biomaterials in connection with the deposition methods. In this research work, the effects of (α-TCP) coating on three metallic substrates in combination with two coating methods were investigated. Three metallic substrates, S316L, Ti-6Al-4V and AZ31, were coated using electrodeposition and plasma-spraying. The characterization, microhardness, corrosion behavior and bioactivity of the coated samples were determined. The characterization of the (α-TCP) coating by XRD and FTIR confirmed the presence of α-TCP. The results showed that the addition of α-TCP coating had improved, hardness, the bioactivity and corrosion resistance significantly. The plasma-sprayed substrates were found to be more effective as they formed less cracks. Thus, α-TCP coated metallic substrates could be considered as a promising method for improving the bio functionality and corrosion resistance in the human body environment.

(Received December 6, 2019; Accepted April 13, 2020)

Keywords: α-tri-calcium phosphate (α-TCP) , Electrodeposition , Plasma Spray, Corrosion , metallic biomaterials.

1. Introduction

Metallic biomaterials are of great interest due to their higher mechanical properties. They have very high tensile strength, fatigue strength, and fracture toughness as compared to ceramics and polymers (Sumita et al., 2004; Patel &Gohil, 2012). Biomedical metals having some degree of toxicity can affect the body and can accumulate with other parts of the body. Metallic implants are also susceptible to bacterial infection (Zhao et al., 2009; Kasemo, 1983). For example, Nickel, Chromium, and Cobalt present in both stainless steel and Cobalt-Chromium alloys produce cytotoxic effects (Hussein et al., 2015). Certain implants containing Ag, Cr, Fe, Mo, Ni and Ta exhibit metallic debris in human body tissues, which may cause the total joint replacements failing (Matusiewicz, 2014). Interaction of Co, metallic Ni, Ni/Cr alloys and Pb with human body could create metal sensitivities, or allergies (Davidson et al., 2007).

---

[*] Corresponding author: durairaj.mech@sathyabama.ac.in

Previously, medical devices were selected based on the material's bulk properties. However, it is now recognized that the surface properties of the device mainly govern its biomedical applications (Roy et al., 2007). The mechanical properties, such as, elastic modulus, ultimate tensile stress, etc. provide sufficient support for the applied mechanical loads. The biological response, on the other hand, is determined by the surface properties, such as protein adsorption or activation, cell adhesion and host response to materials. Most of the metallic biomaterials do not meet the requirements in terms of both surface and bulk properties for biomedical applications. Most metals show poor biocompatibility. An effective way for making a clinically appealing biomaterial is surface modification which can bring biofunctionality of the surface and bulk properties of the base metal (Ikada, 1994; Mohammed et al., 2014; Agarwal, &García, 2019; Anderson et al., 2008). Surface modification offers enhanced biocompatibility, chemical slothfulness, lubricity, sterility, asepsis, thrombogenicity, and hydrophilicity of biomaterial. It also improves the mechanical properties viz. corrosion resistance, surface hardness, Young's modulus and wear resistance. Hence, the biomaterials should maintain the balance between their bulk and surface properties (Mahajan & Sidhu, 2017; Adipurnama et al., 2017).

Some of these coating methods are mechanical methods (such as machining, polishing, and grit-blasting etc.), chemical methods (such as acidic/alkaline treatment, hydrogen peroxide treatment, sol-gel coating, CVD, anodic oxidation, etc.), physical methods (thermal spraying, flame spraying, plasma spraying, high velocity oxy-fuel spraying, physical vapour deposition, ion implantation and deposition, glow charge plasma treatment etc.) and others (surface roughening, surface patterning, 3D printing, injection moulding etc.) (Kulkarni et al., 2014; Liu et al., 2019; Govindarajan&Shandas, 2014; Sidambe, 2014). According to Jemat et al. (2015), a right coating method may provide high impact on the biocompatibility and the mechanical strength. However, there are issues, such as poor long-term adherence of the coating to the substrate material, nonuniformity in thickness of the deposited layer, and variations in crystallinity and composition of the coating. In addition, in the biological systems, the mechanism and effect of corrosion are still in its nascent stage. Very little known is known about its interactions and behaviour with the foreign body (Asri et al., 2017). With the current development in the surface engineering techniques, the fundamental information on material properties, behavior, and the reaction could be uncovered (Asri et al., 2017). The study of corrosion mechanism has been conducted only on a few systems and is essential to conduct more studies to study the influence of a given coating deposition method parameter on corrosion mechanism, for a given combination of deposition method and bioalloy; and similarities and differences in corrosion mechanisms for different coating deposition methods (Lewis, 2017).

Even though some of the recent works on α-TCP coatings had discussion on bioactivity and/ or corrosion resistance of the metallic biomaterials, there is a little information on the applicability of α-TCP for a variety of biomaterials in connection with the deposition methods. The incorporation of α-TCP is expected to improve the bioactivity as well as the corrosion resistance. However, there might be variations in the coating properties due to the fundamental coating parameters (such as the coating technique, coating material composition and properties, coating variables, substrate material composition, and properties etc.), which were very rarely reported in the literature. In this work, the effectiveness of α-TCP coating was investigated on different metallic substrates (SS316L, Ti-6Al-4V and AZ31) using different coating techniques (electro deposition and plasma-spraying) in order to understand its suitability for biomedical applications. The characterization, microhardness, corrosion behavior and bioactivity of the coated samples were determined.

2. Materials, preparation, and coating:

2.1. Materials

Three commercially available surgical grade metal substrates (SS316L, Ti-6Al-4V, and AZ31), calcium nitrate and diammonium hydrogen phosphate (with 99.5% purity level as mentioned by the supplier) were purchased.

2.2. Surface preparation

The metal substrates were initially prepared based on the procedures describe by Lin and Wang (2012), Salman et al. (2013) and Isa et al. (2012) with some modifications. The metal substrates were cut in to square pieces of 1 cm each side. The surface of the metal substrates were polished mechanically with silicon carbide emery sheets (P320 to P1200 grits), followed by etching with acetone, in order to remove the metal oxides and to increase the surface roughness for improving the adhesion between substrates and the HA coating. Etching could thereby improve the corrosion resistance (Gray-Munro et al., 2009). After etching process, the metals substrates were rinsed in distilled water and dried before use.

2.3. Synthesis of α-TCP

α-TCP is used for surface coating material that was synthesized from calcium nitrate and diammonium hydrogen phosphate in the laboratory at International Research Centre, Sathyabama Institute of Science and Technology, Chennai. α-TCP was obtained using the method suggested by Sung et al., (2004) with minor modifications. Separate beakers containing 0.4 M of calcium nitrate and 0.239 M of diammonium hydrogen phosphate each were dissolved in water to make a 500 ml of aqueous solution separately. After dissolving in water, each solution was stirred continuously at 350 rpm for about 5-10 minutes. The aqueous solutions of calcium nitrate and diammonium hydrogen phosphate were then transferred to another beaker in which the diammonium hydrogen phosphate solution was added at a flow rate of 3ml/min to form α-TCP solution. The addition of diammonium hydrogen phosphate was done until the pH value reached to 7. At this time, the solution would become as the milky white colour. The solution was kept for aging overnight for the precipitates to form as shown in Figure 3.4. The solution was then centrifuged at 2500 rpm for 15 minutes at 4°C in order to obtain the concentrated α-TCP solution. The solution was finally heated in an oven (The ILE Co.) at 80°C and crushed into the α-TCP powder.

2.4. Coating by electrodeposition

Electro deposition was carried out based on the procedure followed by Nam et al. (2015) and Kar et al. (2006) with minor modifications using the electro deposition test rig (Make - Aplab-L6430). The electrolyte solution contained 0.4 M of aqueous calcium nitrate and 0.239 M of aqueous diammonium hydrogen phosphate so that Ca/P molar ratio of electrolytic solution would be identical to α-TCP (1.67). S316L, Ti6AL4V and AZ31 substrates were used as the working electrode (cathode) separately over which HA coating was performed. Platinum (anode) was used as the reference electrode. Electro deposition was carried out at constant voltage and current of 5V and 5 mA respectively at room temperature for 2 h. After the coating was performed, the coated substrate was removed from the equipment. The process was repeated for all specimens. The uniformity of coating thickness was assured by maintaining the coating parameters and deposition time. The thickness was verified by measuring the thickness before and after coating at various locations using a micrometer (Insize digital micrometer, with sensitivity of 0.001 mm) to ensure the coating uniformity over the substrate surfaces.

2.5. Coating by plasma-spraying

The plasma spray coating was performed in the plasma spraying machine available at Spraymet Surface Technologies Pvt. Ltd., Bangalore. The synthesized α-TCP powder was fed at 45 gm/min through a nozzle where the α-TCP powder was mixed with plasma of about 1000 °F temperature to make the plasma. At this high temperature, α-TCP powder melts, and accelerates towards the substrate surface. The sprayer (with a spray distance of about 3 in) sprays α-TCP over the metallic substrate to form the coating. The thickness and uniformity were determined by the speed as well as coating time. The plasma spray was performed on S316L, Ti6AL4V and AZ31 substrates. The thickness of the plasma spray coated specimens was verified at different locations of the coated substrates with the help of the micrometer (Insize digital micrometer, with sensitivity of 0.001 mm).

3. Experimentation

3.1. X-ray Diffraction (XRD)

The phase composition of the prepared α-TCP coating was characterized by XRD (Rigaku - SmartLab SE X-Ray Model, available at Vels Institute of Science, Technology and Advanced Studies, Chennai). The XRD was carried out using CuKα radiation (of wavelength 1.5406 Å), with 40 kV and 30 mA at a scan rate of 0.04°. The XRD analysis was obtained in the form of intensity versus the diffraction angle (2θ) for each test sample. After obtaining the XRD plots, they were analyzed to confirm the presence of α-TCP.

3.2. Fourier Transform-Infrared Spectroscopy (FTIR)

The molecular structures of the α-TCP coating were characterized by FTIR analysis (Thermo Fisher Scientific, available at Sathyabama Institute of Science and Technology, Chennai). In FTIR analysis, the α-TCP coating was tested in FTIR spectrum of infra-red (IR) rays and the diffracted rays were detected by an IR detector. The pattern of the diffracted rays was recorded as the reflectance versus the wave number plot for the prepared test specimens. After obtaining the plots, the peaks of the plots were decoded and analyzed to confirm the presence of α-TCP.

3.3. Energy Dispersive X-Ray Spectroscopy Analysis (EDAX)

The elemental compositions of the uncoated and coated samples were recorded with the help of EDAX (Intertek Wilton equipment, available at Sathyabama Institute of Science and Technology, Chennai). The result of the EDAX analysis is the spectra showing peaks corresponding to the elements of the sample which are mapped to the elements. The elemental composition is given as a plot with the list of elements and their percentage. These plots could be used for the understanding of the elemental compositions of different specimens.

3.4. Scanning Electron Microscopy (SEM)

The surface morphologyand apatite-forming ability of the test samples were observed with the help of SEM (CARL ZEISS AG, available at Sathyabama Institute of Science and Technology, Chennai). The cleaned samples of 1 in^2 were placed in the specimen holder in the SEM equipment. The observations were made on the coated samples before and after the apatite formation.

3.5. Microhardness Measurements

The mircrohardness of the uncoated and coated specimens were determined according to the procedure described by Amaravathy et al. (2014a) and Amaravathy et al. (2014b). The testing was carried out in the Vicker'smicrohardness tester (Carl Zeiss Microhardness Tester, available at Sathyabama Institute of Science and Technology, Chennai). The load of 100 g was applied for 5 s and the hardness was determined. At least five hardness measurements were taken in random locations for each uncoated or coated substrate and the average was considered for the characterization.

3.6. Apatite-Forming Ability Test

The apatite-forming ability of the uncoated and HA coated substrates was conducted according to the procedure described by Kokubo and Takadama (2006), Takadama and Kokubo (2008), Li et al. (1992 and Kokubo (1998) with minor modifications. A measured quantity of SBF was poured in a beaker. After heating the solution to 38°C, each test specimen (with 1cm X 1cm open area) was immersed in the SBF. The samples of uncoated and α-TCP coated S316L, Ti6AL4V and AZ31 were soaked separately in the SBF solution as shown in **Fig. 1**. A part of test specimens soaked in SBF is shown in Figure. The fresh SBF was replaced for every 48 hours. After soaking the test specimens at 38°C for different periods, the samples were washed in distilled water gently and dried. The formation of apatite over the sample surfaces were examined with the help of SEM images.

Fig. 1. Samples immersed in Simulated body fluid solution for Apatitte formation test.

3.7. Electrochemical Corrosion

Electrochemical corrosion rates were determined with the help of potentiodynamic polarization cell available at Sathyabama Institute of Science and Technology, Chennai. (Make: Biologic –SP300) The polarization cell is an experimental setup that consists of a voltage regulator unit connected to a computer, and three electrodes (reference electrode, counter electrode, and working electrode) immersed in an electrolytic solution as shown in Fig. 2.

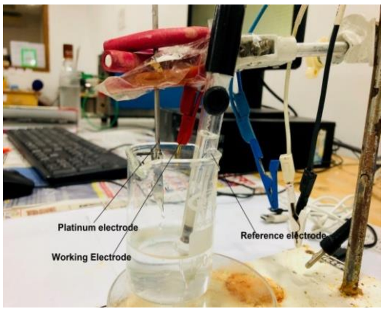

Fig. 2.Electrochemical Polarization Setup.

In this examination, there were three electrodes (platinum as counter electrode; α-TCP coated S316L, Ti6AL4V or AZ31 as the working electrodes and saturated calomel electrode as the reference electrode) used in the polarization cell. These electrodes were immersed in the SBF solution of 100 ml. The coated and uncoated samples of 1cm X 1cm size were considered as the working electrodes. The sample was attached to a holder. The temperature of 38°C was maintained (which is similar to that of a human body). Corrosion rates of the uncoated and coated metallic substrates were determined according to ASTM standards, ASTM G59 and ASTM G102. Electrochemical polarization gives a result in terms of Tafel plots that represent the electrical potential (E) in one axis and the logarithm of absolute current (I) in another axis. The Tafel plots could be used for determining the corrosion rates. In the present investigation, the commercial software was used to plot the electrical potential on the Y axis and the resultant logarithmic current on the X axis. From the plot, corrosion potential (E_{corr}) and corrosion current (i_{corr}) were determined from the cross over point as shown. After determining E_{corr} and i_{corr} values from the Tafel plots, the corrosion rates are calculated from the following equation:

$$\text{Corrosion rate (mm/yr)} = 3.27\text{x}10^{-3}\frac{i_{corr}EW}{\rho}$$

where,

i_{corr} is the corrosion current obtained from Tafel plot (μA/cm^2).

EW is the equivalent weight calculated according to ASTM G102. The equivalent weight and the density of the metallic substrates are shown in Table 1.

ρ is the density of the material (g/cm^3).

Table 1.Equivalent weight and density of substrates.

Material	**Equivalent weight**	**Density (g/cm^3)**	**Reference**
S316L	26.42	7.98	Omrani et al., 2012
Ti-6Al-4V	11.9	4.43	Burnat et al., 2013
AZ31	12.15	1.74	AlHazaa et al, 2015

3.8. Immersion Testing

The immersion testing was carried out based on the procedure according to ASTM G31. The samples (uncoated and coated) were prepared with square shape of 1 in x 1in size according to ASTM G1 standard. The initial weight of each sample was measured and noted. Each sample was then immersed in a separate beaker containing 200 ml of SBF solution. A part of test samples are shown in Fig. 3. The SBF solution was replaced with the fresh SBF solution once a day. After the required immersion period, the sample was taken out of the beaker and rinsed in distilled water, and dried. The final weight of the sample was measured.

Fig. 3.Immersion testing of S316L, Ti6AL4V and AZ31 substrates.

From the initial and final weight before and after the immersion testing, the weight loss (ΔW) of the sample was determined by subtracting final weight from initial weight. This process was repeated for as many samples required to determine the weight loss of the uncoated and coated S316L, Ti-6Al-4V and AZ31 substrates with three replicates and for 25 days. The weight loss (ΔW) could be used to understand the corrosion behavior of the uncoated and coated substrates (Li et al., 2010; Gill et al., 2017; Amaravathy et al., 2014a).

4. Results and discussion

4.1. Characterization

Fig. 4 shows the XRD results of the synthesized α-TCP. In the XRD pattern of the HA coating, the peaks were observed for the 2θ values of 26°, 30°, 32°, 33°, 34°, 40°, 48°, 50°, 54° and 64°, which corresponds to the diffraction planes, namely, (002), (210), (211), (300), (202), (130), (222), (213), (004) and (304), respectively. These 2θ values and their corresponding diffraction planes were compared with the material data available at American Society for Testing and Materials (ASTM) data (JCPDS file no. 9002214) and the standard ICDD no. 84-1998. It was found that all these diffraction peaks correspond to the peak values mentioned in the ASTM material data and therefore the presence of α-TCP was confirmed.

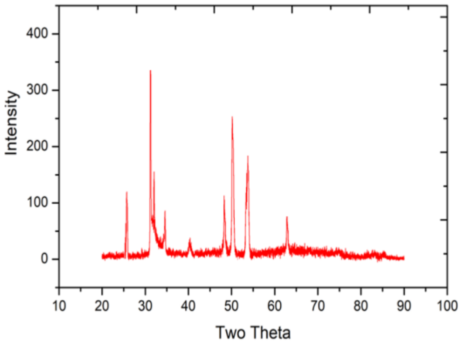

Fig. 4. XRD pattern obtained for the pure α-TCP coating.

In the FTIR image (Fig. 5) vof the α-TCP coating, the pattern of the diffracted rays after diffraction was recorded by varying the wave number and the peaks of the plot were analyzed. The functional groups corresponding to the peaks were identified from the wave number catalogue and marked in the Fig. 5. It was found that the α-TCP powder consisted of hydroxyl group (OH^-), carbonate group (CO_3^{2-}) and phosphate group (PO_4^{3-}). These confirm the presence of α-TCP structures.

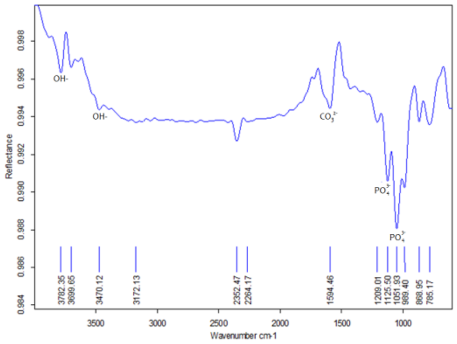

Fig. 5.FTIR Image of α-TCP.

In the results of Vicker'smicrohardness (Fig. 6), it was observed that the microhardness values of the electrodeposited samples were lower than those of the plasma-sprayed samples for S316L, Ti-6Al-4V and AZ31 substrates. Due to the higher hardness value of the plasma-sprayed metallic substrates, the surface of the coating was found to be greater with higher wear strength. Thus, the α-TCP plasma-sprayed samples could withstand for a longer time as compared to those of the electrodeposited samples.

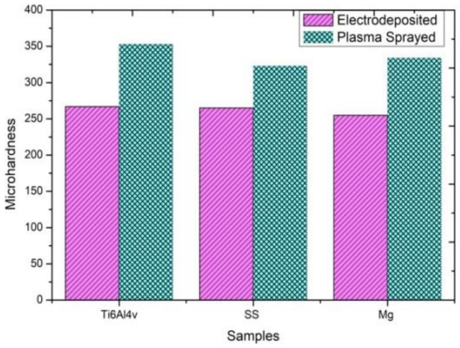

Fig. 6.Microhardness of α-TCP electrodeposited and plasma-sprayed substrates.

The EDAX image (Fig. 7a) showed the presence of O, Na, P, Ca, Cr, Fe and Ni elements in the electrodeposited S316L substrates. The presence of Ti, Al, V, O, Na, P, Cl, and Ca elements in Fig. 7b confirmed the presence electrodeposited Ti-6Al-4V substrates. The image (Fig. 7c) showed the presence of Mg, O, Ca and P elements in the electrodeposited AZ31 substrates. In addition, as α-TCP composed of the elements such as Ca, Ni, O, H, P and N, most of these elements were present in the EDAX images due to the biogrowth of apatite.

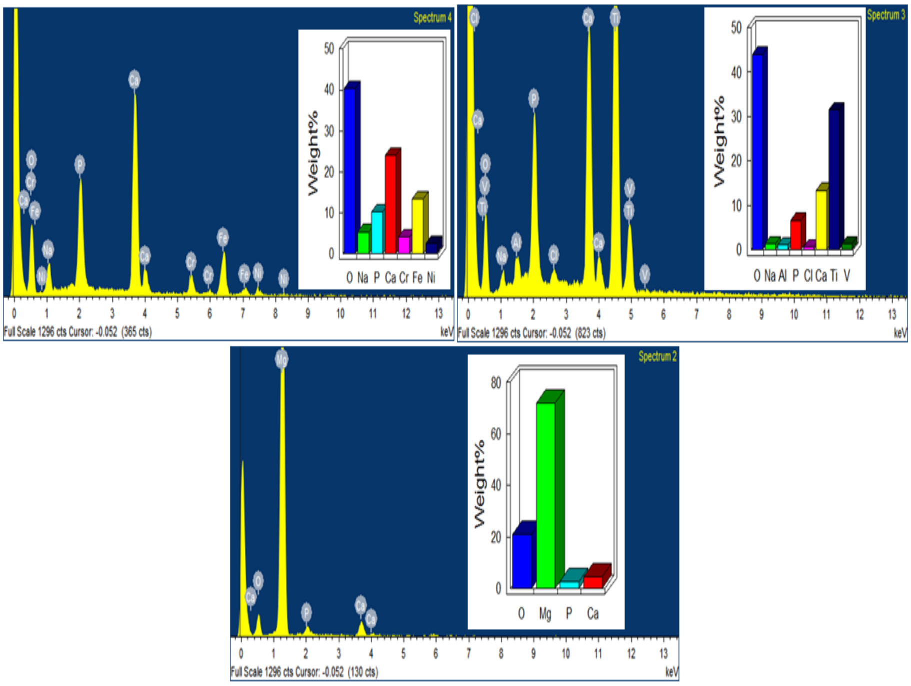

Fig. 7.EDAX Images of Electrodeposited Samples.

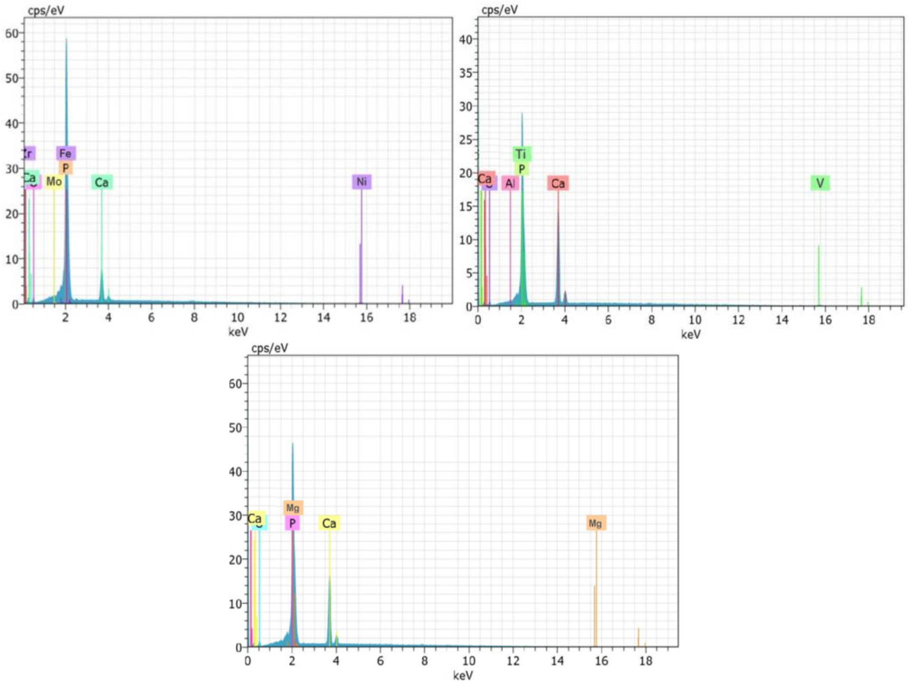

Fig. 8. EDAX Images of Plasma Sprayed Samples.

The EDAX image in Fig. 8a the presence of P, Ca, Mo, Cr, Fe and Ni elements, which confirms the availability of plasma-sprayed S316L substrates. Fig. 8b showed the presence of P, Ca, Ti, Al, O and V elements in the plasma-sprayed TI-6AL-4V substrates. Fig. 8c showed the presence of Ca, Mg, O and P elements, which confirms the plasma-sprayed AZ31 substrates.

4.2. Bioactivity

The bioactivity was evidenced (encircled in Fig. 9) from the SEM images in both the electrodeposited and plasma-sprayed S316L substrates. However, the α-TCP electrodeposited S316L substrate showed the apatite formation in small regions, while the α-TCP plasma-sprayed substrate showed the apatite formation in relatively larger regions. The bioactivity was thus enhanced by α-TCP coating. Corrosion pits were observed in the SEM images of the α-TCP coated samples. The plasma-sprayed S316L substrates showed less number of corrosion pits as compared to those of electrodeposited substrates.

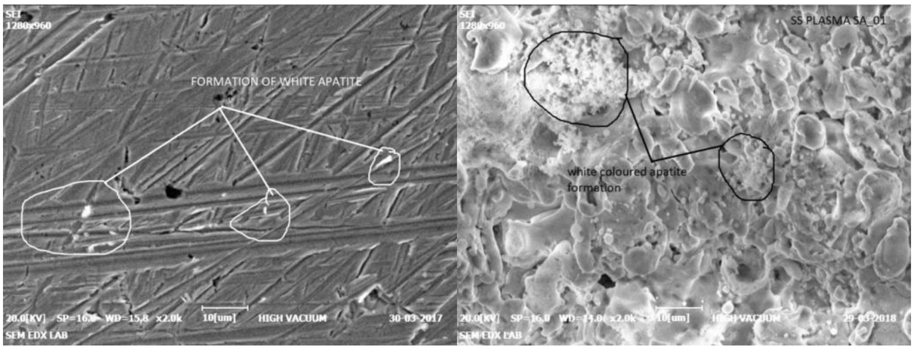

a) *b)*

Fig. 9.In-vitro Characterization of (a) electrodeposited and (b) plasma-sprayed S316L Substrates.

Fig. 10 showed the in-vitro characterization of electrodeposited and plasma-sprayedTi-6Al-4V substrates. The α-TCP electrodeposited and plasma-sprayed Ti-6Al-4V substrates had no micro-cracks. The α-TCP electrodeposited Ti-6Al-4V substrate showed the apatite formation in small regions, where as the α-TCP plasma-sprayed substrate showed the larger portion of the apatite formation. Some corrosion pits were found in the SEM images indicating the start of the corrosion process.

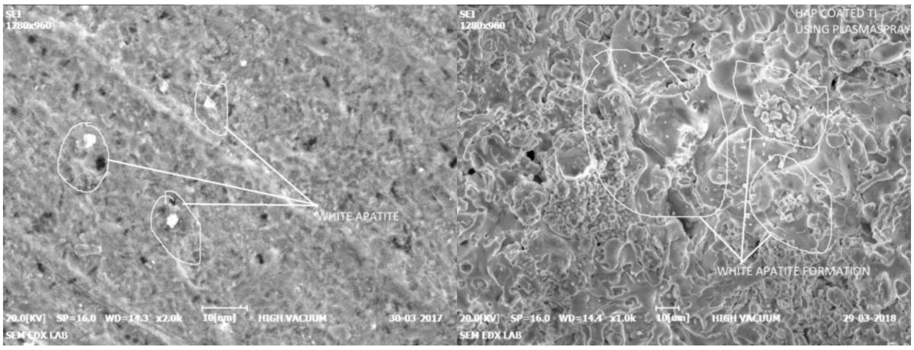

a) *b)*

Fig. 10.In-vitro Characterization of (a) electrodeposited and (b) plasma-sprayed Ti-6Al-4V Substrates.

Fig. 10 SEM image of the α-TCP electrodeposited and plasma-sprayed AZ31 substrates after the apatite formation. Both electro deposition and plasma-spraying of α-TCP indicated the bioactivity by forming the apatite on the AZ31 substrates. However, while the electrodeposited substrate showed the apatite formed at major portion of the substrate, the plasma-sprayed substrates formed relatively low portion of apatite formation. It should also be noted that some micro-cracks and corrosion pits were seen on the surface of the α-TCP electrodeposited AZ31 substrates. In the mean time, the α-TCP plasma-sprayed S316 substrate did not show any such micro-cracks. This revealed that the α-TCP plasma-sprayed S316 substrates showed better corrosion resistance than α-TCP electrodeposited S316 substrates.

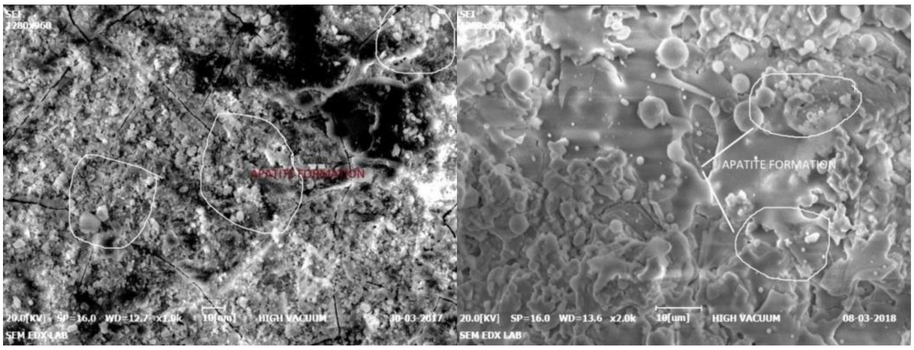

a) *b)*

Fig. 10.In-vitro Characterization of (a) electrodeposited and (b) plasma-sprayed AZ31 Substrates.

4.3. Corrosion Behavior

The polarization curves of the uncoated and α-TCP coated S316L substrates are shown in Fig. 11. The E_{corr}, i_{corr} and corrosion rates of the uncoated as well as α-TCP electrodeposited and plasma-sprayed S316L substrates are shown in Table 2.

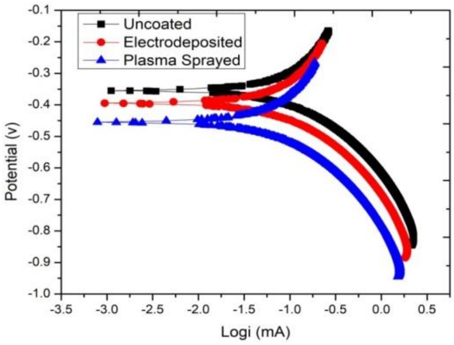

Fig. 11.Electrochemical Polarization Curves of Uncoated and α-TCP Electrodeposited S316L Samples.

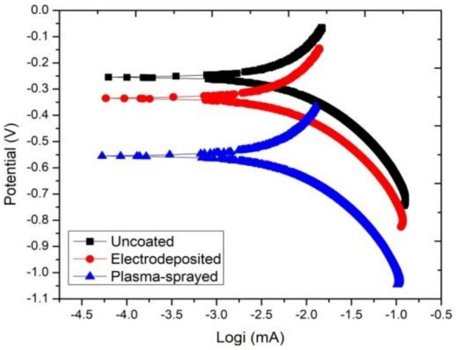

Fig. 12.Electrochemical Polarization Curves of Uncoated and α-TCP Electrodeposited Ti-6Al-4V Alloy Samples.

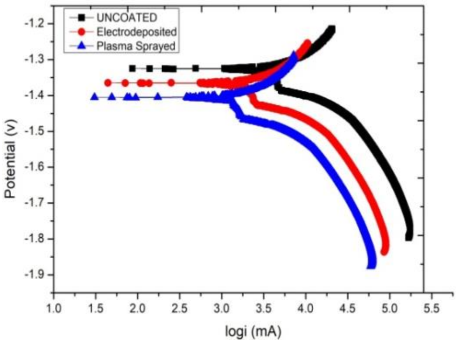

Fig. 13.Electrochemical Polarization Curves of Uncoated and Coated AZ31 Alloy Samples.

Table 2.Corrosion Rates of Uncoated and HA Electrodeposited S316L Samples.

S No	**Sample**	**E_{CORR} (V)**	**I_{CORR} (mA/cm^2)**	**Corrosion Rate (mm/yr)**
1	S 316 L (Uncoated)	-0.342	0.429	0.00465
2	S316 L (Electrodeposited)	-0.371	0.414	0.00449
3	S316 L (Plasma-sprayed)	-0.376	0.412	0.00446
4	Ti-6Al-4V (Uncoated)	-0.326	0.126	0.00111
5	Ti-6Al-4V (Electrodeposited)	-0.416	0.120	0.00105
6	Ti-6Al-4V (Plasma-sprayed)	-0.422	0.117	0.00103
7	AZ31 (Uncoated)	-1.32	105.63	2.412
8	AZ31 (Electrodeposited)	-1.72	79.04	1.805
9	AZ31 (Plasma-sprayed)	-1.89	67.36	1.538

It was found that the E_{corr} values of the α-TCP coated S316L substrates were found to be more negative than those of the uncoated substrates and the i_{corr} values of the α-TCP coated S316L substrates were lower than that of the uncoated substrates. This revealed that the α-TCP coating improved the corrosion resistance of the S316L substrates. The corrosion rate of electrodeposited S316L substrates was found to be 0.00449 mm/yr, which is about 3.4% lower corrosion rate than that of the uncoated S316L substrates. The corrosion rate of plasma-sprayed S316L substrates was 0.00446 mm/yr, which is about 4% lower corrosion rate of the uncoated S316L substrates. Though the variation of corrosion resistance is insignificant, the α-TCP plasma-sprayed S316L substrates produced higher corrosion resistance than that of the electrodeposited S316L substrates.

Both α-TCP electrodeposited and plasma-sprayed Ti-6Al-4V substrates showed more negative E_{corr} values and reduced i_{corr} values than those of the uncoated substrates indicating that the α-TCP coating increased the corrosion resistance. The corrosion rates of the electrodeposited and plasma-sprayed Ti-6Al-4V substrates were found to be 0.00105 mm/yr and 0.00103 mm/yr, which were approximately 4.9% and 6.8% lower than that of the uncoated Ti-6Al-4V substrates (0.00111 mm/yr). The α-TCP coating thus reduced the corrosion rates of Ti-6Al-4V substrates significantly. Among the two coating methods, however, the plasma-sprayed Ti-6Al-4V substrates offered better corrosion resistance as compared to that of the electrodeposited Ti-Al-4V substrates.

It was found that the E_{corr} values of the coated AZ31 substrates were more negative, while the i_{corr} values of the coated substrates were found to be lower as compared to the uncoated substrates. Therefore, the α-TCP coating improved the corrosion behaviour of AZ31 substrates. The corrosion rates of the electrodeposited and plasma-sprayed AZ31substrates were found be 1.804 mm/yr and 1.538 mm/yr, respectively, approximately 25.2% and 36.2% lower than the corrosion rate of the uncoated AZ31 substrates. This result also indicated that, in order to increase the corrosion resistance, the plasma-spraying method of coating was considered to be more effective as compared to the electro deposition method.

5. Conclusions

In this work, the effects of coating on three metallic substrates (S316L, Ti-6Al-4V and AZ31) in combination with two coating methods (electro deposition and plasma-spraying) were investigated. From the results, the following conclusions were made.

The characterization of the α-TCP coating by XRD and FTIR confirmed the presence of α-TCP. The microhardness measurements revealed that the plasma-sprayed samples for S316L, Ti-6Al-4V and AZ31 substrates showed higher Vicker'smicrohardness numbers over the α-TCP electrodeposited samples. The plasma-sprayed samples for S316L, Ti-6Al-4V and AZ31 substrates were found to be rougher than those of the α-TCP electrodeposited samples. While electrodeposited S316L, Ti-6Al-4V and AZ31 substrates showed surface roughness of 5.89, 6.34 and 6.34 µm, respectively, the plasma-sprayed substrates showed surface roughness of 9.53, 9.02 and 9.53 µm, respectively. The micro hardness values of α-TCP plasma-sprayed S316L, Ti-6Al-4V and AZ31 substrates are 21.8%, 32.2% and 30.9%, respectively, which are higher than those of the electrodeposited substrates.

The apatite-forming ability of the α-TCP coated S316L, Ti-6Al-4V and AZ31 substrates was investigated after 7 days of immersion in SBF. The SEM images evidenced the formation of the apatite over all the metal substrates. Thus, the bioactivity of the metal substrates was improved due to the addition of α-TCP coating. The plasma-sprayed substrates were found to be more effective as they formed less cracks.

The corrosion behaviour of the α-TCP coated S316L, Ti-6Al-4V and AZ31 substrates were investigated using electrochemical corrosion testing and immersion testing. While the corrosion resistance of the α-TCP electrodeposited and plasma-sprayed S316L substrates were improved by 3.4% and 4%, respectively, those of Ti-6Al-4V and AZ31 substrates were increased by 5.4% and 7.2%, and 25.2% and 36.2%, respectively. Immersion testing revealed the similar behaviour in which the weight loss was reduced after the α-TCP coating on the metallic substrates. In all three cases, the α-TCP plasma-sprayed S316L, Ti-6Al-4V and AZ31 substrates showed lower weight loss as compared to those of the electrodeposited substrates.

Thus, from the results it is concluded that the addition of α-TCP coating over the metallic substrates could be considered as a promising method for improving the bio functionality and corrosion resistance in the host human body.

References

[1] I. Adipurnama, M.-C. Yang, T. Ciach, B. Butruk-Raszeja, Biomaterials Science **5**(1), 22 2017).

[2] R. Agarwal, A. J. García, APrinciples of Regenerative Medicine, 651 (2019).

[3] S. Agarwal, J. Curtin, B. Duffy, S. Jaiswal, Materials Science and Engineering: C **68**, 948 016).

[4] M. Akmal, M. A. Hussain, H. Ikram, T. Sattar, S. Jameel, J. Y. Kim, J. W. Kim, Ceramics International **42**(3), 3855 (2016).

[5] M. Akmal, M. A. Hussain, H. Ikram, T. Sattar, S. Jameel, J. Y. Kim, F. A. Khalid, J. W. Kim, Ceramics International (2015),

[6] B. Aksakal, O. S. Yildirim, H. Gul, J. Fail.Anal. Prevent. **4**(3), 17 (2004).

[7] S. L. Aktug, I. Kutbay, M. Usta, Journal of Alloys and Compounds**695**, 998 (2017).

[8] A. N. AlHazaa, M. S. El-Sayed, H. S. Abdo, Int. J. Electrochem. Sci, **10**(542), 5433 (2015).

[9] V. A. Alves, R. Q. Reis, I. C. B. Santos, D. G. Souza, T. D. F. Gonçalves, Corrosion Science **51**(10), 2473 (2009)

[10] P. Amaravathy, S. Sathyanarayanan, S. Sowndarya, N. Rajendran, Ceramics International **40**(5), 6617 (2014).

[11] P. Amaravathy, S. Sowndarya, S.Sathyanarayanan, N. Rajendran, Surface and Coatings Technology **244**, 131 (2014).

[12] K. Ananth, J. Sun, J. Bai, International Journal of Molecular Sciences **19**(8), 2340 (2018).

[13] J. M. Anderson, A. Rodriguez, D. T. Chang, SeminImmunol**20**(2), 86 (2008).

[14] U. Anjaneyulu, U. Vijayalakshmi, Materials Letters **189**, 118 (2017).

[15] V. E. Annamalai, S. Kavitha, S. A. Ramji, The Open Materials Science Journal**8**(1), 2014.

[16] RB Durairaj ,S Ramachandran Int. journal of Electrochemical science , ESG publications. Vol 13 PP4841-4854 **(2018)**

[17] R. I. M. Asri, W. S. W. Harun, M. Samykano, N. A. C. Lah, S. A. C. Ghani, F.Tarlochan, M. R. Raza, Materials Science and Engineering C**77**, 1261 (2017).

[18] R. I. M. Asri, W. S. W. Harun, M. Samykano, N. A. C. Lah, S. A. C. Ghani, F. Tarlochan, M. R. Raza, Materials Science and Engineering C **77**, 1261 (2017).

[19] A. Atrens, M. Liu, N. I. Z. Abidin, NMater. Sci. Eng. B **176**, 1609 (2011).

[20] H. M. Ayu, S. Izman, R. Daud, G. Krishnamurithy, A. Shah, S. H. Tomadi, M. S. Salwani, Procedia Engineering **184**, 399 (2017).

[21] R. Azari, H. R. Rezaie, A. Khavandi, Ceramics International, 2019)

[22] A. Bagno, C. Di Bello, Journal of Materials Science: Materials in Medicine **15**(9), 935 (2004).

[23] D. A. Basketter, G. Briaticovangosa, W. Kaestner, C. Lally, W. J. Bontinck,Contact Dermatitis **28**, 15 (1993).

[24] S. Bauer, P. Schmuki, K. von der Mark, Progress in Materials Science **58**(3), 261 (2013).

[25] K. Bazaka, N. Ketheesan, M. V. Jacob, J. Nanosci. Nanotechnol.**14**, 8087 (2014).

[26] R. M. Bergman, MRS bulletin **30**(7), 540 (2005).

[27] A. Besinis, S. D. Hadi, H. R. Le, C. Tredwin, R. D. Handy, Nanotoxicology**11**(3), 327 017).

[28] H. R. A. Bidhendi, M.Pouranvari, Metallurgical and Materials Engineering, 2012.

[29] A. Bigi, E. Boanini, B. Bracci, A. Facchini, S. Panzavolta, F. Segatti, L. Sturba, Biomaterials **26**(19), 4085 (2005).

[30] D. J. Blackwood, Corrosion Reviews **21**, 2 (2003).

[31] M. Bohner, J. J. Lemaitre, Biomaterials **30**, 2175 (2009).

[32] H. S. Brar, M. O. Platt, M. Sarntinoranont, P. I. Martin, PM. V. Manuel, JOM **61**, 31 (2009).

[33] R. A. Buchanan, E. E. Stansbury, Handbook of Environmental Degradation of Materials **87**, (2012).

[34] B. A. Burnat, M. A. Walkowiak-Przybyło, T. A. Błaszczyk, L. Klimek, Acta of Bioengineering and Biomechanics **15**(1), 2013.

[35] H. Chen, C. Wang, X. Yang, Z. Xiao, X. Zhu, K. Zhang, X. Zhang, Materials Science and Engineering C **70**, 1047 (2017).

[36] Q. Chen, G. A. Thouas, Materials Science and Engineering R **87**, 1 (2015).

[37] R B Durairaj , S Ramachandran International Journal of Chemical Sciences (2016) **14(4)** 2157-2163.

[38] Y. Chen, Z. Xu, C. Smith, J. Sankar, Actabiomaterialia**10**(11), 4561 (2014).

[39] Durairaj R B , Ramachandran S Research Journal of Pharmaceutical, Biological and Chemical Sciences **7(5)** 2423-2427. (2016)

[40] R B Durairaj , G Mageshwaran , Jeyajeevahan J , Arvind T, J Hemanandh , Metin Kok , Digest Journal of Nanomaterials and Biostructures **14(2)** 343-350 (2019).